The interplay of osteogenesis and hematopoiesis: expression of a constitutively active PTH/PTHrP receptor in osteogenic cells perturbs the establishment of hematopoiesis in bone and of skeletal stem cells in the bone marrow

Sergei A. Kuznetsov,[1] Mara Riminucci,[2,3] Navid Ziran,[1] Takeo W. Tsutsui,[1] Alessandro Corsi,[4] Laura Calvi,[5] Henry M. Kronenberg,[5] Ernestina Schipani,[5] Pamela Gehron Robey,[1] and Paolo Bianco[1,3,4]

[1]Craniofacial and Skeletal Diseases Branch, National Institute of Dental and Craniofacial Research, National Institutes of Health, Bethesda, MD 20892
[2]Dipartimento di Medicina Sperimentale, Università dell'Aquila, 67010 L'Aquila, Italy
[3]Parco Scientifico Biomedico San Raffaele, 00161 Rome, Italy
[4]Dipartimento di Medicina Sperimentale e Patologia, Università "La Sapienza," 3 00161 Rome, Italy
[5]Endocrine Unit, Massachusetts General Hospital, and Harvard Medical School, Boston, MA 02114

The ontogeny of bone marrow and its stromal compartment, which is generated from skeletal stem/progenitor cells, was investigated in vivo and ex vivo in mice expressing constitutively active parathyroid hormone/parathyroid hormone–related peptide receptor (PTH/PTHrP; caPPR) under the control of the 2.3-kb bone-specific mouse Col1A1 promoter/enhancer. The transgene promoted increased bone formation within prospective marrow space, but delayed the transition from bone to bone marrow during growth, the formation of marrow cavities, and the appearance of stromal cell types such as marrow adipocytes and cells supporting hematopoiesis. This phenotype resolved spontaneously over time, leading to the establishment of marrow containing a greatly reduced number of clonogenic stromal cells. Proliferative osteoprogenitors, but not multipotent skeletal stem cells (mesenchymal stem cells), capable of generating a complete heterotopic bone organ upon in vivo transplantation were assayable in the bone marrow of caPPR mice. Thus, PTH/PTHrP signaling is a major regulator of the ontogeny of the bone marrow and its stromal tissue, and of the skeletal stem cell compartment.

Introduction

Postnatal bone marrow is composed of two distinct tissues and hosts a dual system of stem cells. Hematopoietic tissue proper includes a range of maturing hematopoietic cells originating from the proliferation, commitment, and differentiation of blood-borne hematopoietic stem cells (HSCs) and progenitors, which seed the marrow (Morrison et al., 1995). The stroma, which permits hematopoiesis by providing appropriate environmental cues, is instead derived from the same lineage as cartilage and bone cells, and is established during bone development (Bianco and Riminucci, 1998). Postnatal marrow stroma also includes a hierarchy of skeletal stem cells (SSCs; also referred to as stromal stem cells or mesenchymal stem cells) and progenitors (Friedenstein, 1980; Owen and Friedenstein, 1988; Bianco and Robey, 2000, 2004), which give rise to different kinds of skeletal cells, contribute to skeletal growth, maintain skeletal mass, and convey the remarkable potential for repair and regeneration with which bone is endowed (Bianco et al., 1999). SSCs and committed osteoprogenitors (OPs) are both found in the clonogenic subset of adherent bone marrow

S.A. Kuznetsov and M. Riminucci contributed equally to this paper.

Correspondence to Pamela Gehron Robey: probey@dir.nidcr.nih.gov; or Paolo Bianco: p.bianco@flashnet.it

N. Ziran's present address is Dept. of Orthopaedics, School of Medicine and Dentistry, University of Rochester, Rochester, NY 14642.

T.W. Tsutsui's present address is Dept. of Pharmacology, The Nippon Dental University, School of Dentistry at Tokyo, Tokyo 102-8159, Japan.

L. Calvi's present address is Endocrine/Metabolism Unit, Strong Memorial Hospital, School of Medicine and Dentistry, University of Rochester, Rochester, NY 14642.

Abbreviations used in this paper: caPPR, constitutively active PPR; CFE, colony-forming efficiency; CFU-F, colony-forming unit–fibroblast; FD, fibrous dysplasia; H&E, hematoxylin and eosin; HA/TCP, hydroxyapatite/tricalcium phosphate; HSC, hematopoietic stem cell; microCT, microcomputerized tomography; MMA, methyl methacrylate; OP, osteoprogenitor; PPR, PTH/PTHrP receptor; PTH/PTHrP, parathyroid hormone/parathyroid hormone–related peptide; SSC, skeletal stem cell; tg, transgenic; wt, wild-type.

The Journal of Cell Biology, Vol. 167, No. 6, December 20, 2004 1113–1122
http://www.jcb.org/cgi/doi/10.1083/jcb.200408079

cells, which are nonhematopoietic, nonendothelial, nonphagocytic, and fibroblastic in habit, and therefore regarded as stromal in nature. These cells, referred to as clonogenic stromal cells or colony-forming unit–fibroblasts (CFU-Fs), initiate the growth of discrete colonies upon plating at low cell density. Presently, SSCs and OPs cannot be distinguished from one another by a defined surface phenotype. Assessments of CFU-F frequencies in marrow through appropriate clonogenic efficiency assays thus estimate the size of the total population of stem cells/progenitors in a marrow sample, without directly probing the presence, or estimating the specific frequency, of SSCs. Nonetheless, SSCs and OPs are endowed with distinct growth and differentiation potential, as is revealed by in vivo transplantation assays (Bianco et al., 1999). SSCs are those single CFU-Fs that generate progeny in culture that are capable of forming bone and nonhematopoietic elements of marrow upon ex vivo expansion and subsequent transplantation (Bianco and Robey, 2004). By establishing a complete ectopic bone/marrow organ that survives for the recipient animal's lifespan, these cells demonstrate multipotency and self-renewal; they are established in culture as marrow stromal cells, and, after many population doublings ex vivo, regenerate marrow stromal cells in vivo. OPs, in contrast, are those single CFU-Fs that generate progeny capable of forming bone, but not a complete bone/marrow organ, upon transplantation in vivo (Chailakhyan et al., 1978; Kuznetsov et al., 1997). In mice, ~10% of CFU-Fs represent in vivo assayable SSCs, and ~25% represent differentiation-restricted (committed) OPs (Chailakhyan et al., 1978).

Mechanisms that regulate hematopoietic marrow development in bone, establishment of stroma, and the ontogeny of SSCs and committed OPs have remained largely unexplored. Their interplay with developmental events that establish the shape, structure, size, and mass of bones remains, likewise, to be elucidated. These mechanisms must operate in the context of endochondral bone formation, the organogenic process by which most bones, and the marrow that fills them, develop. Endochondral bone formation is characterized by a precisely timed sequence of tissue transitions (Streeter, 1949). Formation of the embryonic anlagen, which is made of hyaline cartilage, is followed by the emergence of primary ossification centers in its midst. Here, chondrocytes hypertrophy, and their matrix calcifies and is invaded by blood vessels and osteogenic cells migrating from the surrounding perichondrium. Calcified cartilage is resorbed by osteoclasts and then replaced by bone (the primary spongiosa). With continuing resorption of the primary spongiosa, the primary center splits into two opposite physes (growth plates), in each of which cartilage maturation to hypertrophy and calcification, and subsequent remodeling into bone, continue as long as new chondrocytes are generated in the growth plate. As chondrocyte proliferation/differentiation fuels longitudinal bone growth during postnatal life, the physes are separated by increasing amounts of bone and marrow, consisting of hematopoietic cells held in a network of stromal cell processes (Streeter, 1949). Cartilage matures to hypertrophic and calcified cartilage, before it is resorbed and replaced by bone. Bone formed by this process is then resorbed and replaced by newer bone (secondary spongiosa), and this is ultimately replaced by marrow. Therefore, during endochondral bone formation a similar principle of timed remodeling of one tissue into another governs both the formation of metaphyseal bone to replace cartilage and the formation of marrow to replace metaphyseal bone.

Substantial advances have been made in the identification of genes regulating cartilage growth, maturation, and replacement by bone during endochondral ossification (de Crombrugghe et al., 2001). Little insight has been gained, however, into mechanisms that establish, through the same organogenic process, the bone marrow and its dual stem cell system, or the critical, functional interplay of hematopoietic and stromal cells. The pivotal role of parathyroid hormone/parathyroid hormone–related peptide (PTH/PTHrP) signaling in regulating cartilage-based transitions in endochondral bone formation was highlighted by development of PTHrP- and PTH/PTHrP receptor (PPR)–deficient mice (Karaplis et al., 1994; Lanske et al., 1996). In both models, ablation of PPR signaling caused early cessation of chondrocyte proliferation, accelerated maturation to hypertrophic chondrocytes, premature ossification in growth plates, and severe dwarfism. Conversely, enhanced PPR signaling in chondrocytes has the opposite effect; that is, it causes delayed maturation. Constitutively active PPR (caPPR), usually the result of an H223R mutation, causes Jansen-type metaphyseal chondrodysplasia (Schipani et al., 1995, 1996). Targeted expression of caPPR in cartilage rescues the phenotype of PTHrP knockout mice (Schipani et al., 1997). When targeted to chondrocytes in the PTHrP-sufficient mouse, expression of caPPR caused a marked delay in maturation to hypertrophy (Schipani et al., 1997). Lack of invasion of prenatal cartilage anlagen in these mice delayed formation of the primary spongiosa and of a marrow cavity.

Targeting of caPPR to cells of the osteogenic lineage (Col1-caPPR) in mice results in another distinct phenotype, dominated by marked increases in bone mass and turnover in postnatal long bones (Calvi et al., 2001). Here, we show that Col1-caPPR induces a complex derangement in the ontogeny, kinetics, and biological properties of the bone marrow stromal system. By regulating the timed transition between bone and marrow during bone growth, PPR regulates the establishment of the hematopoietic stroma and of stromal stem cells therein.

Results

Col1-caPPR delays establishment of hematopoiesis in bone

At 2 wk, the marrow cavity was well formed in the femur and tibia of wild-type (wt) mice, and clearly detectable by X-ray imaging. In contrast, the marrow cavity of Col1-caPPR transgenic (tg) mice was reduced to a small mid-diaphyseal region because of a marked extension of the primary spongiosa from the metaphyses into the diaphyses (Fig. 1, a and b). Histologically, the excess bone of tg mice was composed of bone trabeculae lined by normal-appearing osteoblasts. The area between the trabeculae was occupied by fibroblastoid cells, blood vessels, and osteoclasts, but devoid of hematopoietic cells, at 2 wk. Marrow was confined to a small diaphyseal region corre-

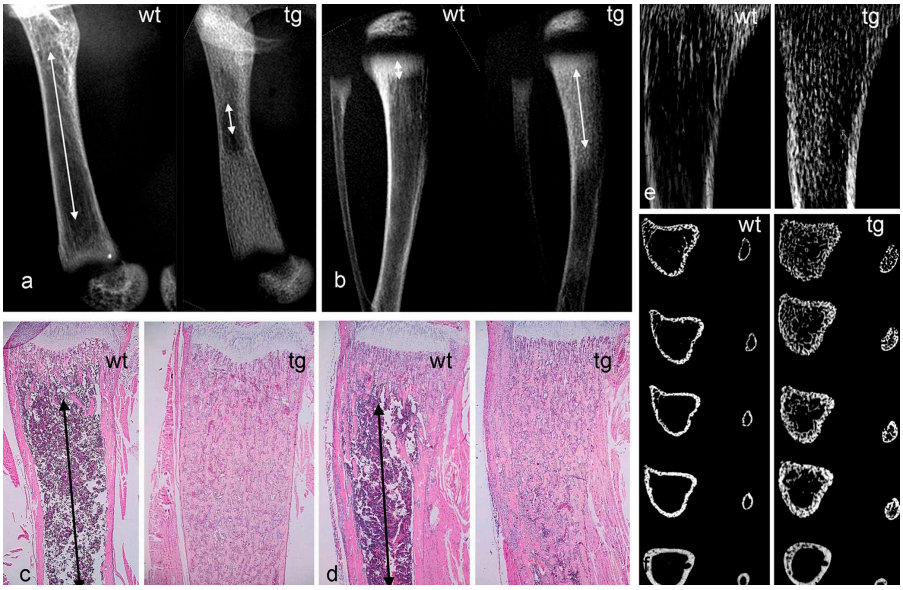

Figure 1. **Impaired development of the marrow cavity and hematopoietic tissue in long bones of COL1-caPPR mice.** (a) High resolution radiograms of the femurs of wt and tg mice at 2 wk. Note the marked difference in length of the marrow cavity (arrows). (b) High resolution radiograms of tibiae and fibulae of wt and tg mice at 2 wk. Note the different lengths of the primary spongiosa (arrows). (c and d) Histological sections of the distal metaphysis of the femur (c) and proximal metaphysis of the tibia (d) at 2 wk. Red marrow extends to the metaphyseal end of the primary spongiosa in wt mice (arrows), but only medullary bone is present in tg mice. (e and f) High resolution contact microradiography (e) and microCT analysis (f) of tibiae at 2 wk. The excess medullary bone formed in tg mice is obvious with both techniques. MicroCT demonstrates that the normal partition between cortical bone and marrow space is lost in tg mice, and that both are replaced by a continuous plexus of cancellous bone. Sections extend from 0.5 to 2.5 mm below the physis.

sponding to the radiographically detectable marrow cavity in tg mice, whereas it extended from one metaphyseal spongiosa to the other in wt long bones (Fig. 1, c and d).

High resolution microradiographs of 100-μm sections clearly showed the formation of excess (medullary) bone in the metaphyseal and upper diaphyseal regions of tg tibiae (Fig. 1 e). Microcomputerized tomography (microCT) analysis of tibiae and fibulae demonstrated that a distinct, bone-free marrow cavity was well apparent 0.5 mm below the physis in both wt bones (Fig. 1 f). In tg mice, the marrow cavity was partially occupied by bone trabeculae for 2–3 mm below the physis in the tibia, and no cavity was discernible in the fibula. In both bones of tg mice, a continuous plexus of cancellous bone trabeculae effaced the spatial and structural distinctions between marrow space and cortical bone observed in wt mice (Fig. 1 f).

Col1-caPPR impairs marrow adipogenesis

Either red (hematopoietic) or yellow (adipose) marrow occupies specific regions in the mammalian skeleton (Tavassoli and Yoffey, 1983). In mice, the entire marrow cavity of the calcaneum is occupied by yellow marrow at skeletal maturity. Histological analysis of the calcaneum at 2 wk and 3 mo revealed that a transient phase of active hematopoiesis (red marrow) precedes the establishment of yellow marrow in wt mice (Fig. 2 a). At 2 wk, the marrow cavity of the calcaneum was well defined and contained abundant hematopoietic cells and developing adipocytes, recognizable by their typical multivacuolar morphology (Fig. 2, c and inset), similar to what is observed during phases of active adipogenesis in other species. No hematopoiesis or adipogenesis was seen in 2-wk-old tg calcaneum, in which a continuous trabecular bone structure was seen instead (Fig. 2, b and d). At 3 mo, formation of a thick bony cortex and yellow marrow filling the cavity were complete in wt mice (Fig. 2 e). In contrast, a marked excess of bone filled the marrow cavity in tg calcaneum, and only rare adipocytes were scattered in the narrow vascular spaces remaining patent (Fig. 2 f).

Temporal changes in bone and marrow structure in Col1-caPPR mice

Radiographic analysis at multiple time points demonstrated an obvious evolution of the phenotype in tg mice over time (Fig. 3). Remodeling of the extended primary spongiosa into a sec-

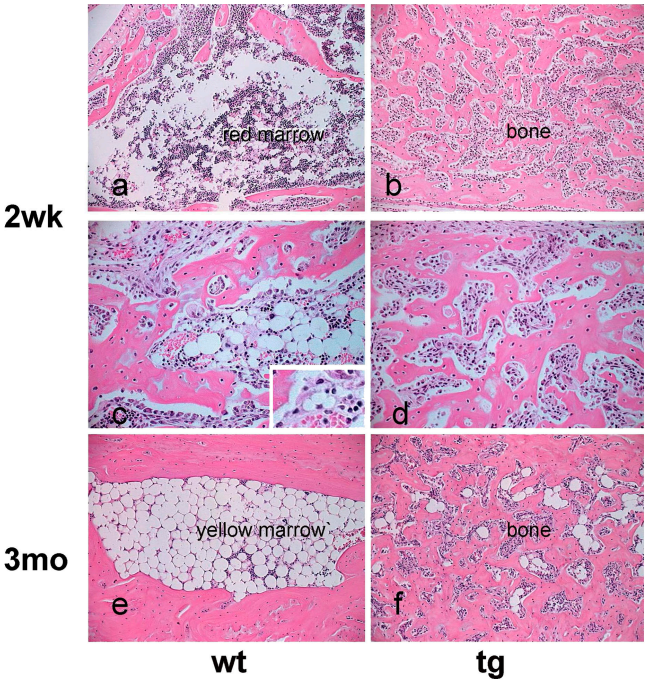

Figure 2. **Impaired development of adipose (yellow) marrow in COL1-caPPR mice.** Histology of the calcaneum at 2 wk and 3 mo. At 2 wk, the wt marrow cavity contains red hematopoietic marrow (a) with scattered adipocytes, and frequent multivacuolar, developing adipocytes (c and inset). In tg mice, a distinct cavity is not observed, hematopoiesis and adipocytes are absent, and an excess of bone is present (b and d). At 3 mo, hematopoiesis is no longer present, and the marrow cavity is filled with mature adipocytes in wt mice (e). No cavity is present in tg mice, and only rare adipocytes are found in narrow vascular spaces interrupting the continuity of the excess bone (f).

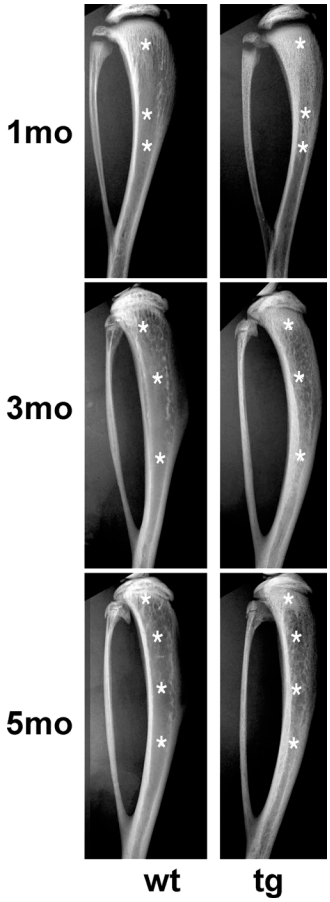

Figure 3. **Relative growth of marrow cavities with respect to bone over time.** High resolution radiograms of tibia and fibula at 1, 3, and 5 mo. At 1 mo, a much longer primary spongiosa is observed in tg mice than in wt mice. In continuity with the extended primary spongiosa, abundant trabeculae are detected in the medullary cavity of the diaphysis. Corresponding regions in wt tibia show a bone-free marrow cavity. At 3 mo, a dense primary spongiosa is still present in the tg tibia, albeit much reduced in length compared with what is observed at 1 mo. Below this region, a marrow cavity is discernible. However, it is occupied by a dense meshwork of bone trabeculae. Corresponding regions in the wt tibia show a bone-free marrow cavity. A similar pattern is observed at 5 mo. Asterisks mark corresponding regions in the primary spongiosa, metaphysis, and diaphysis in radiograms of wt and tg mice.

ondary spongiosa was obvious at 1 mo, and continued thereafter. This process generated increasing amounts of marrow, while leaving behind a system of trabeculae, which extended well into the diaphysis of tg mice. Corresponding regions of the same wt long bones featured a fully formed marrow cavity devoid of trabecular structures. With time, a marrow cavity of near-normal length was established at 4–5 mo in tg mice.

Occurrence of multiple remodeling cycles in the extended primary spongiosa ("medullary bone") originally formed in lieu of marrow space in tg mice was confirmed by histological studies (Fig. 4). Between 2 wk and 5 mo, fluorescence microscopy of hematoxylin and eosin (H&E)–stained sections visualized complex arrays of cement/reversal lines (each marking an individual remodeling cycle) within the medullary trabeculae of tg mice (Fig. 4 d). At the same time, a marked change in the morphology of cells residing on trabecular surfaces and within intertrabecular areas was observed. Al-

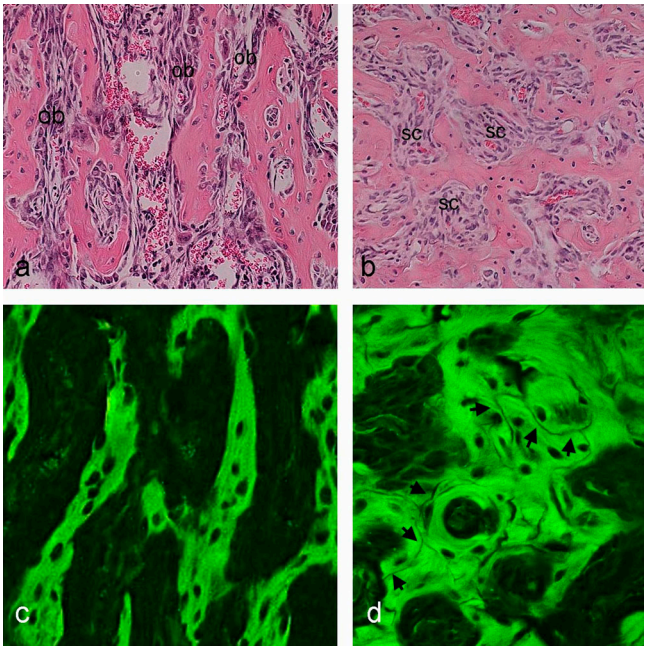

Figure 4. **Transient fibrous dysplastic phase in bone and marrow of Col1-PPR mice.** (a and b) Transmitted light views of standard H&E-stained sections of the proximal metaphysis of the tibia at 2 wk and 3 mo. The medullary bone is lined by typical cuboidal osteoblasts (ob) at 2 wk (a), and, although excessive, it is otherwise histologically normal. In contrast, morphologically typical osteoblasts cannot be recognized, and only spindle-shaped cells (sc) fill the spaces between trabeculae at 3 mo (b). The orientation of trabeculae is more haphazard, giving the tissue a dysplastic appearance. (c and d) Fluorescence microscopy images of the same sections. No cement lines (marks of bone remodeling events) are seen at 2 wk (c), which is consistent with the primary nature of the medullary bone. A complex pattern of cement lines (which remain nonfluorescent in H&E-stained sections) is seen at 3 mo (d, arrows), testifying to the occurrence of multiple remodeling cycles.

though osteoblasts of normal morphology lined the surface of primary medullary bone trabeculae at 2 wk (Fig. 4 a), cells associated with medullary bone at 3 mo were uniformly spindle shaped and fibroblastic in habit (Fig. 4 b). Together, cell morphology, accumulation of fibrous tissue, and abnormal bone structure compounded a dysplastic pattern reminiscent of human fibrous dysplasia (FD; Riminucci et al., 1997, 1999). The relative length of the region occupied by dysplastic bone and fibrous tissue decreased over time and was limited to a narrow metaphyseal region at 4 mo. At 5 mo, a hematopoietic marrow extended to the physis proper. However, throughout the metaphysis, an overt excess of trabecular bone was demonstrated histologically in tg mice, matching the radiographic analysis.

Reduced frequency and enhanced ex vivo expansion of CFU-F in skeletally mature Col1-caPPR mice

Because a significant alteration in postnatal development of marrow was a key phenotypic trait of tg mice, we wanted to determine whether these changes affected the composition and functional properties of the marrow stromal cell population. To this end, stromal cell strains were established in culture from wt and tg mice at 5 mo (the age when a distinct marrow cavity had formed from which stromal cells could be harvested from

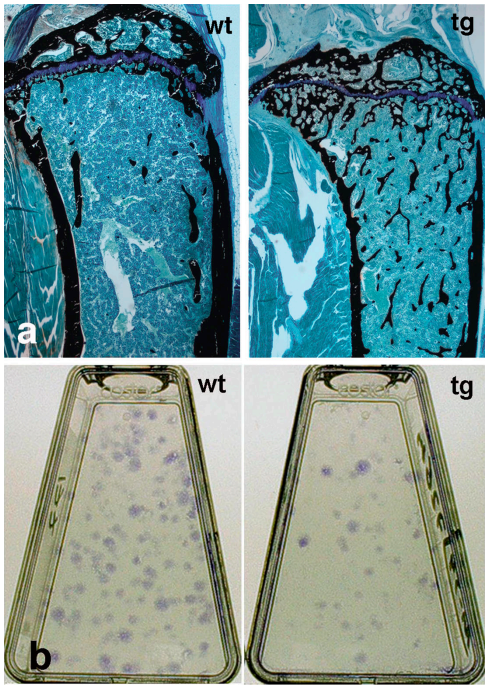

Figure 5. **Histology of the bone/marrow organ and CFU-F frequency in mice at skeletal maturity.** (a) Histology of the proximal metaphysis of the tibia in wt and tg mice at 4.5 mo. Hematopoietic marrow now fills the marrow cavity up to the physis in both wt and tg mice. A marked excess of trabecular bone is observed in tg mice compared with in wt mice (undecalcified MMA sections, von Kossa staining). (b) Representative primary cultures of cells established at clonal density from wt and tg mice. Note the higher number of colonies (CFU-F) in wt cultures.

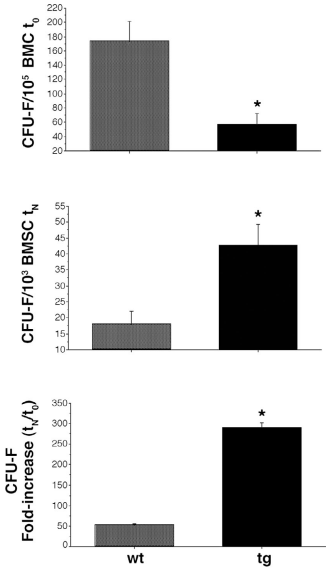

Figure 6. **Frequency and expansion capabilities of CFU-F.** (top) Frequency of CFU-F at the time of explantation (t_0). Results shown as number of colonies per 10^5 nucleated bone marrow cells (mean of triplicate determinations per mouse). The tg marrow is reduced in CFU-F, relative to the wt marrow (analysis of variance [ANOVA], Scheffe's F test 309.16* [significant at 95%], $P < 0.0001$). (middle) Frequency of CFU-F at the end of ex vivo expansion (day 17, t_N). Results shown as number of colonies per 10^3 stromal cells (mean of triplicate determinations per two cell strains per genotype). Strains of tg mice are enriched in total CFU-F, relative to strains of wt mice (ANOVA, Scheffe's F test 94.03* [significant at 95%], $P < 0.0002$). (bottom) Fold increase in CFU-F over the culture period was calculated as the ratio of the total number of CFU-Fs at the end of the culture period to the total number of CFU-Fs in the marrow explants. Results based on triplicate determinations in duplicate experiments (ANOVA, Scheffe's F test 124.52* [significant at 95%], $P = 0.02$). (top, middle, and bottom) Error bars indicate SD of the mean.

tg mice). The structure of the bones from which cells were derived in culture was examined by high resolution radiographic analysis. Corresponding bones of mice of the same age as those used for establishing cell cultures were subjected first to the same kind of radiographic analysis, and then to histological analysis. This procedure demonstrated a much higher amount of trabecular bone associated with the marrow of tg mice compared with that of wt mice (Fig. 5 a). No difference in the cellular composition of hematopoietic tissue was histologically apparent in tg mice.

Primary cultures were initiated by plating $\sim 8 \times 10^7$ nucleated bone marrow cells. Because SSCs and OPs are both included in the clonogenic subset of stromal cells (CFU-Fs), the frequency of CFU-Fs at the time of explantation was determined by a colony-forming efficiency (CFE) assay (CFE_{t0}), as the number of CFU-Fs per 10^5 nucleated bone marrow cells. This demonstrated a significantly lower CFE (three- to fourfold) in tg mice than in wt mice (Figs. 5 b and 6 a). Based on the CFE assay, the total number of CFU-Fs plated in each high density culture was calculated ($CFU\text{-}F_{t0}$).

In primary culture, tg strains demonstrated a shorter doubling time than wt strains (32.2 vs. 35.5 h, respectively). Over 17 d in culture, tg and wt strains underwent 12.6 and 11.5 population doublings, respectively. At the end of ex vivo expansion, total cell yield per initially plated CFU-F was 2.3-fold higher for tg strains than for wt strains (6.8×10^3 vs. 2.9×10^3, respectively). The frequency of CFU-Fs at the end of culture (before in vivo transplantation) was assessed by enumerating the number of CFU-Fs, which was done by plating 10^3 cells per strain in 25-cm^2 flasks (CFE_{tN}). At this time, the frequency of CFU-Fs in the total population had become significantly higher (more than twofold) in tg strains than in wt strains (Fig. 6 b). The total numbers of CFU-Fs in wt and tg strains at the end of culture were then determined based on CFE_{tN} and total cell yield, and ratioed to the total number of explanted CFU-Fs in each strain ($CFU\text{-}F_{tN}/CFU\text{-}F_{t0}$). This revealed a mean 52.7-fold increase in CFU-Fs in wt strains, and an average 290.2-fold increase in CFU-Fs in tg strains (an approximately sixfold increase in tg strains compared with wt strains; Fig. 6 c). Hence, threefold as many total cells, but approximately sixfold as many CFU-Fs per single, originally explanted CFU-F, were obtained for tg strains compared with wt strains over the same time in culture. The CFU-Fs from tg mice expanded in culture to a greater extent, and generated more CFU-Fs per total number of stromal cells, than those from wt mice.

The presence of OPs, but lack of SSCs, in the marrow of skeletally mature Col1-caPPR mice

The ability of wt and tg cell strains to generate a complete heterotopic bone organ and establish a hematopoietic microenvironment was tested with two different in vivo transplantation assays. We

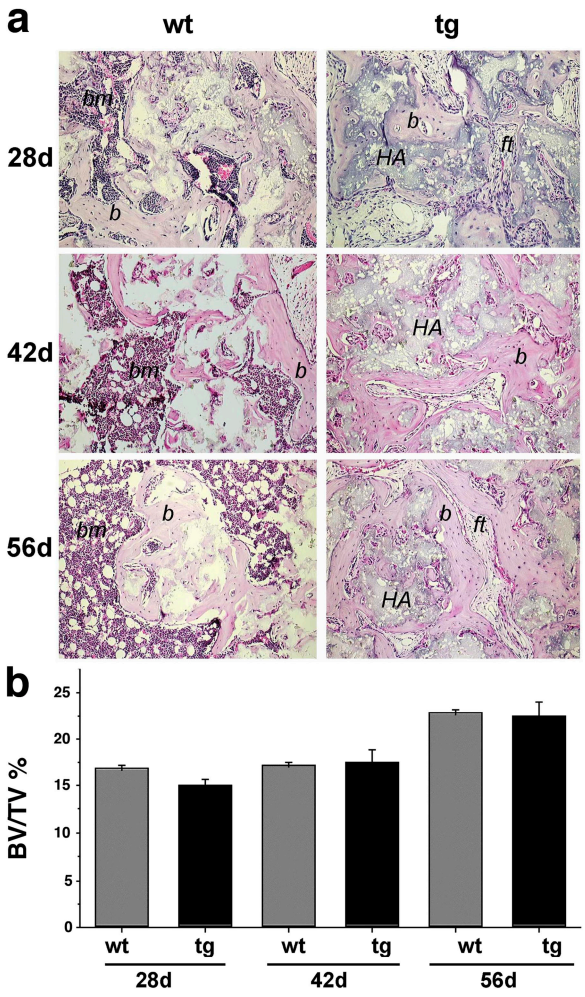

Figure 7. **Osteogenic potential of stromal strains.** (a) Histology of ectopic ossicles formed subcutaneously in immunocompromised mice by strains derived from wt and tg mice transplanted with an osteoconductive carrier (HA/TCP particles; HA). Formation of bone (b) and marrow (bm) is obvious in transplants of wt cells at 28, 42, and 56 d. Adipocytes in the hematopoietic marrow are evident at 42 and 56 d. Formation of bone, but not of red marrow, is obvious in transplants of tg cells at 28, 42, and 56 d. Adipocytes are not formed, and only fibrous tissue (ft) fills the spaces between bone surfaces. (b) Histomorphometric assessment of the amount of bone (bone volume/total volume; BV/TV %) formed in ectopic ossicles did not reveal differences between wt and tg strains at any time point. A similar increase in the amount of bone was observed at 56 d compared with earlier time points in wt and tg transplants. Error bars indicate SD of the mean.

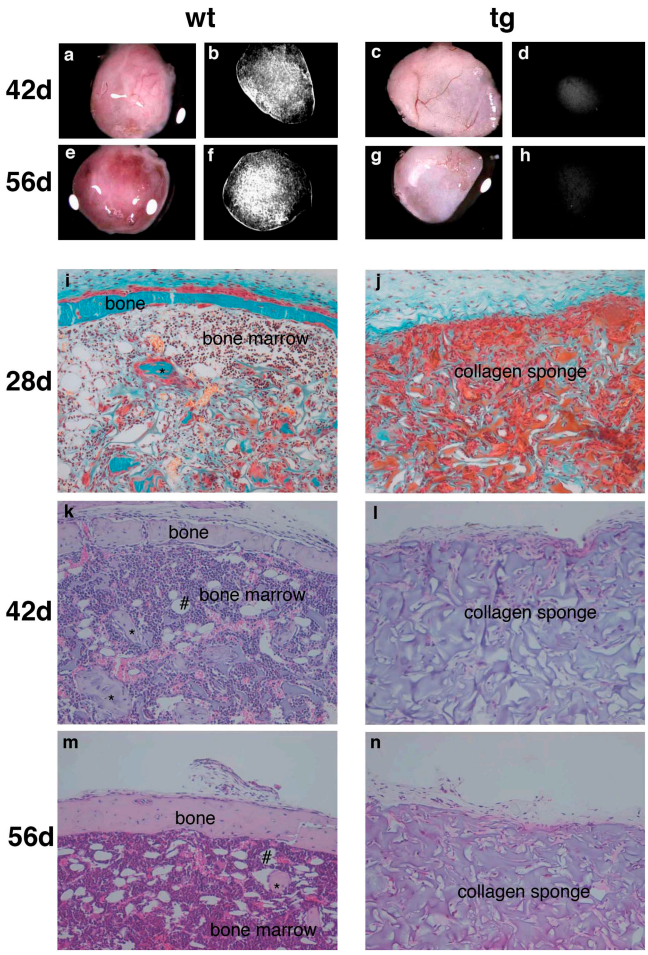

Figure 8. **Gross, radiographic, and histological analysis of subcutaneous transplants of stromal strains in conjunction with collagen sponges.** Gross appearance of the transplants generated by wt (a and e) and tg (c and g) strains harvested at 42 (a and c) and 56 d (e and g). Hematopoiesis gives a red color to wt transplants (a and e), whereas the collagen sponge remains pale gray in spite of vascularization (well apparent in c) in tg transplants (c and g). High resolution radiograms of the same structures for wt (b and f) and tg (d and h) transplants. Bone formation is readily detected in wt transplants (b and f), and even a distinct bony cortex is easily resolved in the ectopic ossicles. No bone was formed by tg cells (d and h). (i and j) Nondecalcified sections stained with Goldner's trichrome stain. (k–n) Paraffin sections stained with H&E. (i–n) Examination of wt transplants at 28 (i), 42 (k), and 56 d (m) revealed the progressive formation of a complete heterotopic ossicle, including a bony cortex and a medullary cavity with trabecular bone (*), and the establishment of a complete hematopoietic marrow. Fully mature adipocytes (#) are well apparent by day 42. Neither bone nor a hematopoietic marrow was present at any time point in tg transplants (j, l, and n).

performed transplants using either a mineral phase (hydroxyapatite/tricalcium phosphate [HA/TCP]) or a nonmineralized, collagenous carrier. The two carriers differ with respect to their osteoconductive properties. Whereas HA/TCP facilitates bone deposition by cells competent for bone formation by providing a preexisting mineralized scaffold (Damien and Parsons, 1991), collagen, per se, does not. In 12 out of 12 transplants made with wt strains and HA/TCP, bone, hematopoietic tissue, and adipocytes were evident at all time points. In contrast, bone and fibrous tissue, but neither hematopoietic tissue nor marrow adipocytes, were formed in 12 out of 12 transplants of tg strains with HA/TCP (Fig. 7 a). The amount of bone formed in the transplants was assessed by histomorphometry and was found to be essentially the same for wt and tg strains at all time points (Fig. 7 b).

Under nonosteoconductive conditions (transplants in collagen sponges), in 12 out of 12 transplants, wt strains formed complete ossicles, composed of a shell of cortical bone and a marrow cavity with bone trabeculae; complete hematopoiesis (granulo-, erythro-, and megakaryopoiesis); and adipocytes (Fig. 8). Early developmental phases of bone and marrow formation (deposition of bone by osteoblasts, adipogenesis, establishment of a sinusoidal vascular bed, and removal of the collagen carrier) were well apparent in wt transplants harvested at 28 d, and formation of a fully structured ossicle was complete at 56 d. In contrast, in spite of the high number of CFU-Fs

transplanted, tg strains consistently failed to establish a heterotopic bone organ upon transplantation (no ossicle formation was observed in 12 out of 12 transplants of tg strains; Fig. 8).

Equal numbers of cells were used for all transplants. Based on the frequency of CFU-Fs determined at the end of the culture period (CFE_{tN}), the number of CFU-Fs that were actually transplanted was calculated to be 3–4 $\times$ 10^4 for wt strains, and 8–9 $\times$ 10^4 for tg strains. The absolute number of transplanted CFU-F was approximately twofold higher for tg strains compared with wt strains. This ruled out the possibility that the impaired ability of tg strains to establish a complete heterotopic bone organ in vivo was caused by an insufficient number of transplanted CFU-Fs, among which OPs and SSCs are found.

These results indicate that OPs, assayable in vivo by transplantation with an osteoconductive carrier (HA/TCP), were present in both tg and wt CFU-F populations. Considering that fewer CFU-Fs were present in tg marrow than in wt marrow, and that tg and wt strains formed similar volumes of bone with HA/TCP in vivo, a greater potential for bone formation could be estimated for tg CFU-Fs than for wt CFU-Fs. Assayable multipotent cells (SSCs), defined as cells able to regenerate a complete heterotopic bone/marrow organ in vivo, regardless of the osteoconductive properties of the carrier used (HA/TCP vs. collagen), were represented in the wt CFU-F population, as expected. In contrast, SSCs were either present in insufficient number, or absent altogether, in the tg CFU-F population. The greater expansion ex vivo of the tg CFU-F population compared with that of the wt CFU-F population was therefore not associated with multipotency in vivo. These results are consistent with a proliferative effect of the transgene on committed OPs, which are endowed with some inherent potential for expansion but are neither multipotent nor self-renewing (that is, they represent transit amplifying, committed progenitors; Bianco and Robey, 2004).

Discussion

The transition from bone to marrow is altered in Col1-caPPR mice

Targeted expression of caPPR in the osteogenic lineage significantly perturbs the development of the bone marrow. Normal remodeling of the primary spongiosa into hematopoietic marrow during longitudinal bone growth suggests the transition from a tissue where PPR is abundantly expressed (i.e., the primary spongiosa; Lee et al., 1993) to a tissue where global PPR expression is low to undetectable (i.e., the bone marrow; Lee et al., 1994; Calvi et al., 2001). In Col1-caPPR mice, constitutive activity of PPR in the primary spongiosa results in generation of excess bone in the presumptive marrow space, at the expense of the developing marrow cavity. As a consequence of expression of caPPR in osteogenic cells, bone formation in the primary spongiosa is enhanced, whereas establishment of marrow is delayed. This is associated with a reduced hematocrit in mice 1–3 mo old (unpublished data).

The hematopoietic marrow includes specific hematopoiesis-supporting stromal cell types (Friedenstein et al., 1974; Tavassoli and Yoffey, 1983), which must be established during the transition from the primary spongiosa to hematopoietic marrow. These include, as a major cell type, reticular cells (Westen and Bainton, 1979), which share several phenotypic traits with osteogenic cells (Bianco and Riminucci, 1998), establish close physical contacts with hematopoietic cells (Westen and Bainton, 1979; Bianco and Boyde, 1993), and are able to convert to marrow adipocytes during postnatal life (Bianco et al., 1988). Adipose conversion of reticular cells underlies the formation of yellow marrow at specific anatomical sites (Tavassoli and Yoffey, 1983), a process impaired, as we have shown, in Col1-caPPR mice. The developmental origin of reticular cells (and of the marrow adipocytes arising from them) has not been fully elucidated, but may be rooted in a local adaptation of osteogenic cells during bone organogenesis (Bianco et al., 1999; Bianco and Robey, 2000). Our observations suggest that as a consequence of caPPR expression in osteogenic cells, the establishment of differentiated stromal cell phenotypes such as reticular cells and adipocytes is perturbed, in the context of the delayed establishment of a marrow cavity and hematopoiesis.

The frequency and function of CFU-Fs are altered in Col1-caPPR mice

The clonogenic subset of adherent stromal cells (CFU-Fs) contains a hierarchy of progenitors that can be assayed by in vivo transplantation and that include a subset of multipotent, self-renewing SSCs (which generate bone and nonhematopoietic marrow elements upon transplantation), as well as a larger subset of committed osteogenic progenitors (which generate bone but do not support marrow formation upon transplantation) (Friedenstein, 1980, 1990; Owen and Friedenstein, 1988; Bianco and Robey, 2000, 2004).

We have shown that at 5 mo, there were fewer CFU-Fs in the stroma of tg mice, but they exhibited a greater expansion potential, than in wt mice. Committed OPs were present within the CFU-F pool and assayable in vivo in tg mice: tg strains formed bone when transplanted with an osteoconductive carrier (HA/TCP). However, the stroma of tg mice contained no assayable multipotent SSCs: only bone, and no hematopoiesis-supporting stroma or adipocytes, was formed by tg stromal strains when they were transplanted with an osteoconductive carrier; neither bone nor marrow was formed when the same strains were transplanted with a nonosteoconductive carrier. Obviously, an osteoconductive phase facilitates the deposition of bone by cells that are fully competent for osteogenesis (Begley et al., 1993). Conversely, collagen sponges lack osteoconductive properties and are removed from the transplant during deposition of bone (Holmbeck et al., 1999). Thus, different osteogenic performances, perhaps ascribed to distinct subsets of cells, are probed in transplantation assays with the two different carriers.

Col1-caPPR mice are deficient in postnatal SSCs

Neither prenatal skeletal patterning and development, nor postnatal osteoblast differentiation and function, appear to be de-

fective in Col1-caPPR mice. This implies that the skeleton of tg mice develops from a normal repertoire of fetal skeletal progenitor cells, and that the observed deficit of CFU-Fs harbored in postnatal marrow is related to developmental events inherent in bone marrow organogenesis, most of which is postnatal in mouse long bones and is perturbed and delayed, as we have shown, in Col1-caPPR mice.

The differences in frequency and properties of tg and wt CFU-Fs at 5 mo are indeed established through a markedly different in vivo history of bone as an organ. BrdU labeling and in situ hybridization studies have shown that between 2 wk and 3 mo, increased cell proliferation expands the pool of osteogenic cells in the metaphyses of tg long bones (Calvi et al., 2001). As a result, preosteoblastic, spindle-shaped cells expressing multiple osteogenic markers accumulate in trabecular spaces of tg mice (Calvi et al., 2001). Later, when marrow stroma becomes directly assayable, a deficit of CFU-Fs (and an absence of assayable multipotent SSCs) is observed in tg mice compared with wt mice.

Targeted expression of the transgene in committed osteogenic cells is fully consistent with a proliferative effect in the same cells, but it would imply, per se, that there are no changes in the number or function of "uncommitted" SSCs. The deficit of assayable SSCs in Col1-caPPR mice, in contrast, implicates them as direct or indirect targets of the transgene effect, which depends on the activation of an osteoblast-specific promoter. This supports the view that SSCs may be at least partially committed to osteogenic differentiation, and thus represent an integral part of the osteogenic lineage, rather than being uncommitted cells (Bianco et al., 1999; Satomura et al., 2000).

Because self-renewal is a defining property of stem cells, it would be expected that the size of the SSC population in the postnatal marrow of tg mice would not be affected by an enhanced rate of proliferation in cells of the osteogenic lineage, whether they included the multipotent SSCs or not. However, a deficit in SSCs may be established through inadequate self-renewal; for example, if the number of cell divisions evoked by the effect of the transgene were to exceed the self-renewal capacity of SSCs. The magnitude of self-renewal of SSCs may be tuned to the relatively low rate of bone turnover compared with the magnitude of self-renewal of blood or epidermis, for example. Self-renewal itself is hardly an absolute property, and failure of self-renewal may be ultimately observed in a variety of tissues after prolonged phases of accelerated turnover. Indeed, an increase in proliferative activity and in remodeling cycles is observed in the bones of tg mice during the medullary bone phase, before establishment of a CFU-F–deficient marrow.

Alternatively, inadequate self-renewal may be explained based on current models of asymmetric kinetics of stem cell–dependent populations (Sherley, 2002). In these models, self-renewing and non–self-renewing types of cell divisions (asymmetric vs. symmetric) may occur in stem cells in a stochastic fashion (Watt and Hogan, 2000). The relative frequency of one type of division versus the other determines preservation, expansion, or consumption of the stem and progenitor cell compartments (Sherley, 2002). One could thus speculate that the transgene may alter the frequency of asymmetric versus symmetric division of SSCs, leading to expansion of the compartment of committed OPs and consumption of SSCs proper. Consistent with this interpretation, we observed that expansion of tg CFU-Fs was not the same as that of wt CFU-Fs, with more CFU-Fs being generated per initial clonogenic cell.

SSCs that would self-renew normally at a constant rate would continue to replenish a compartment of committed OPs, which would overexpand as an effect of the transgene, and sustain unabated medullary bone formation. Thus, inadequate self-renewal of stem cells might explain why the skeletal phenotype of tg mice resolves over time. Calvi et al. (2001) have otherwise documented the persistence of transgene expression in osteogenic/stromal cells of tg mice at 3 mo (when establishment of a marrow cavity is well underway), dispelling the silencing of the transgene as an alternative explanation for the timed clearance of medullary bone in caPPR mice.

The interplay between HSCs and SSCs in the marrow

Calvi et al. (2003) have shown that tg osteogenic/stromal cells appear capable of supporting HSCs with greater efficiency than their wt counterparts. As a result, the compartment of HSCs, but not of hematopoietic progenitors and progeny thereof, is expanded in tg mice at 3 mo. In skeletally mature tg mice, differentiated osteogenic/stromal cells in the marrow cavity support hematopoiesis in vivo and in vitro (Calvi et al., 2003), whereas establishment of hematopoietic marrow is delayed in vivo, and SSCs capable of reforming hematopoiesis-supporting cells upon expansion ex vivo and transplantation in vivo are not assayable among stromal cells. Expression of caPPR in the osteogenic lineage may thus result in different effects on HSC support versus the support of HSC progeny and hematopoiesis proper. In addition, it results in opposing effects on the two different stem cell compartments in bone marrow, HSCs and SSCs. In tg mice, increased numbers of HSCs, and delayed birth and maturation of hematopoietic progenitors, are mirrored in the osteogenic system by a deficiency of assayable SSCs and a prolonged, sustained expansion of committed progenitors. A competitive interdependence of hematopoiesis and osteogenesis at the organ level is obvious in many instances of development and disease, such as the development of inappropriate porosity of bone caused by expansion of hematopoietic tissues in congenital hemolytic anemias (Bianco and Riminucci, 1998). Our data extend the competitive relationship of the two "strange bedfellows" (bone and marrow) to the level of stem cells. It follows that a precisely timed modulation of osteogenesis is critical not only for the establishment of marrow cavities and hematopoiesis, but also for the establishment, at the same time, of an adequate pool of SSCs in marrow, in a precise balance with the size of the HSC compartment. Appropriate modulation of PPR signaling, made impossible by caPPR in osteogenic cells, is essential for this critical switch in bone and marrow organogenesis. Thus, PTH/PTHrP signaling is a major regulator of the ontogeny of marrow and its stromal tissue, and of the SSC compartment.

FD-like changes in bone and marrow of Col1-caPPR mice

We have also shown that a transient dysplastic phase occurs during bone growth in Col1-caPPR mice, closely reminiscent

of changes observed in human diseases noted for derangements in the PPR signaling pathway. These diseases include hyperparathyroidism (Bianco and Bonucci, 1991) and FD of bone (OMIM [Online Mendelian Inheritance in Man] 174800), a genetic disease in which Gsα, a downstream mediator of PPR signaling, is constitutively active because of somatic mutations (Riminucci et al., 1997). In these conditions, as in Col1-caPPR mice, fibroblast-like cells with the phenotype of OPs accumulate around bone trabeculae and replace normal marrow tissue. Interestingly, stromal strains obtained from human FD marrow, like those derived from Col1-caPPR mice, contain skeletal progenitors that only form bone and fibrous tissue, and fail to establish the hematopoietic microenvironment and adipocytes upon in vivo transplantation (Bianco et al., 1998). The histological similarities between the transient fibrous dysplastic phase of Col1-caPPR mice and a human disease rooted in a dysfunction of the same signaling pathway are thus matched by similar behavior of skeletal progenitors when assayed in vivo. Col1-caPPR mice may represent a unique model of the disease, noted as a disease of the stromal stem/progenitor cell system (Bianco and Robey, 1999). Important predictions as to the role of PPR signaling and its downstream mediators in regulating SSC kinetics can be made based on analysis of Col1-caPPR mice and are currently being tested by correlative studies of human SSCs in FD of bone.

Materials and methods

Col1-caPPR mice

Previously, mice were generated in which the mouse 2.3 Col1A1 promoter (bone specific) was linked to 1,880 bp encoding the constitutively active PPR-H223R sequence, along with 750 bp of the cloning vector pcDNAI (Calvi et al., 2001). Tg male mice were bred with wt female FVB/N mice, and litters were harvested at various time points after birth. All studies were performed under institutionally approved animal protocols.

Transgene analysis

Genotyping was done as described previously (Calvi et al., 2001). Genomic DNA was extracted and purified from tail clippings using a commercial kit (QIAGEN), and 2 μl was diluted in 50 μl of PCR master mix (Roche Diagnostics). PCR was performed using a forward primer from the receptor sequence (5′-CACCTGCCCTGCTACAGGAAGAG-3′; nucleotides 423–445 from GenBank/EMBL/DDBJ under accession no. U22409) and a reverse primer from the pcDNA1 vector in the transgene (5′-TTCCACCACTGCCTCCCATTCATC-3′). The samples were heated at 94°C for 1 min; and 30 cycles were performed at 94°C for 30 s, 58°C for 45 s, 72°C for 1 min, and 72°C for 3 min for termination. PCR products resolved by electrophoresis yielded a 350-bp product present only from genomic DNA from tg mice.

Skeletal imaging

Radiographic images of long bones were obtained (MX-20 Specimen Radiography System; Faxitron X-ray Corp.) at an energy of 30 kV for 90 s with X-OMAT TL film and processed by an automated X-ray film developer (model M35A; Eastman Kodak Co.).

Microradiographic analysis was done on undecalcified bones that were dehydrated in ethanol and embedded in an epoxy resin (Bianco et al., 1985). 100–200-μm sections were generated with a microtome equipped with a rotating diamond knife (model HM3505S; Leica). Contact microradiographs were prepared using an X-ray generator (XRG 3000; Ital Structures), operated at 12 kV and 20 mA for 15 min, and high resolution film (Eastman Kodak Co.). Fixed films were observed with a microscope (Axiophot; Carl Zeiss MicroImaging, Inc.).

Tibiae of 2-wk-old mice were analyzed by microCT (ScanCo microCT 10; ScanCo Medical) with 15-μm resolution. Images (at 1,024 by 1,024 pixels) were obtained using a microfocus X-ray beam (7-μm spot size) at 50 kVp, 8 W (160 microAmps).

Histology

Lower limbs from mice at 2 wk and 2, 3, 4, and 5 mo were fixed in 4% formaldehyde in PBS, pH 7.4. Samples were either undecalcified and processed for methyl methacrylate (MMA) embedding or decalcified in neutral solutions of 10% EDTA and embedded in paraffin. MMA sections were stained with von Kossa/Giemsa or Goldner's trichrome stain. Paraffin sections were stained with H&E and viewed with transmitted light or by fluorescence microscopy to visualize bone remodeling cycles (cement lines; Bradbeer et al., 1994).

Cell culture, CFE, and ex vivo expansion

The entire marrow content of six long bones (two femora, two tibiae, and two humeri) was harvested from 4.5-mo-old mice by flushing with α-MEM containing 20% lot-selected FBS, 2 mM glutamine, 100 mU/ml penicillin, and 100 μg/ml streptomycin sulfate (Biofluids, Inc.).

Single cell suspensions were made by repeated pipetting and passage through syringe needles of decreasing gauge and through a cell strainer (Becton Dickinson) to remove aggregates. The frequency of CFU-F (CFE) in the marrow at 5 mo was estimated by plating the cells at clonal density (10^6 cells per 25-cm^2 flask). Nonadherent cells were removed after 4 h by extensive washing, and adherent cells were incubated with medium containing 10^7 nucleated guinea pig marrow cells (irradiated with 6,000 cGy) as feeder cells. Cultures were fixed on day 9 with absolute methanol and stained with methyl violet, and colonies (>50 cells) were counted using a dissecting microscope (Kuznetsov and Gehron Robey, 1996). Colonies were counted using four cultures per animal, generated from two wt and four tg mice. Statistical evaluation was performed with analysis of variance and Scheffe's F test.

Cultures of stromal cells for ex vivo expansion were established from equal numbers of total nucleated bone marrow cells ($\sim 8 \times 10^7$ cells). Cells were expanded by serial passage and harvested on day 17 (P3). At the end of ex vivo expansion, 10^3 cells from each strain were plated in 25-cm^2 flasks, and CFE was assessed again as described in the previous paragraph.

In vivo transplantation assays

The ability of stromal strains from wt and tg mice to recapitulate a bone/marrow organ was assessed with in vivo transplantation assays (Krebsbach et al., 1997). Ex vivo expanded cells were aliquoted at 2×10^6 and pelleted at 1,000 *g*. Half were resuspended in 1 ml of growth medium, allowed to attach to 40 mg of HA/TCP particles (100–200 μm; Zimmer), and embedded in a secondary vehicle (fibrin gel). The other half was resuspended in 30–50 μl of growth medium and loaded into collagen sponges (Gelfoam; Upjohn). Constructs were transplanted subcutaneously into 8–15-wk-old female *bg-nu/nu-xid* mice (Harlan Sprague Dawley) and harvested at 4, 6, and 8 wk, fixed, X-rayed, and either decalcified and processed for paraffin embedding or processed undecalcified for MMA embedding. Histological sections were stained with H&E (paraffin sections) or Goldner's trichrome (MMA sections). The amount of bone formed was determined in undecalcified sections by measuring the total bone volume per tissue volume with a semiautomatic image analyzer (IAS 2000; Delta System), as described previously (Corsi et al., 2003). Comparisons between groups were performed by one-way analysis of variance, and post hoc comparison was performed with Scheffe's F test.

We thank Dr. Bruno Koller for help with microCT studies.

The support of Telethon Fondazione Onlus (grant E.1029), Istituto Superiore di Sanità Programma Nazionale Cellule Staminali, Ministero Istruzione Università Ricerca, and the European Union (Genostem) (to P. Bianco, M. Riminucci, and A. Corsi) is gratefully acknowledged, as is the support of the National Institutes of Health (grants AR044855, for the initial generation of the tg mice [to H.M. Kronenburg, E. Schipani, and L. Calvi], and Z01 DE00380-20 [to P. Gehron Robey, S.A. Kuznetsov, N. Ziran, and T.W. Tsutsui]).

Submitted: 12 August 2004
Accepted: 21 October 2004

References

Begley, C.T., M.J. Doherty, D.P. Hankey, and D.J. Wilson. 1993. The culture of human osteoblasts upon bone graft substitutes. *Bone.* 14:661–666.

Bianco, P., and E. Bonucci. 1991. Endosteal surfaces in hyperparathyroidism: an enzyme cytochemical study on low-temperature-processed, glycol-methacrylate-embedded bone biopsies. *Virchows Arch. A Pathol. Anat. Histopathol.* 419:425–431.

Bianco, P., and A. Boyde. 1993. Confocal images of marrow stromal (Westen-Bainton) cells. *Histochemistry.* 100:93–99.

Bianco, P., and M. Riminucci. 1998. The bone marrow stroma in vivo: ontogeny, structure, cellular composition and changes in disease. *In* Marrow Stromal Cell Culture. M.A. Owen and J.N. Beresford, editors. Cambridge University Press, Cambridge, UK. 10–25.

Bianco, P., and P. Robey. 1999. Diseases of bone and the stromal cell lineage. *J. Bone Miner. Res.* 14:336–341.

Bianco, P., and P.G. Robey. 2000. Marrow stromal stem cells. *J. Clin. Invest.* 105:1663–1668.

Bianco, P., and P.G. Robey. 2004. Skeletal stem cells. *In* Handbook of Adult Stem Cells. R. Lanza, editor. Elsevier Acedemic Press, San Diego. 415–424.

Bianco, P., Y. Hayashi, G. Silvestrini, J.D. Termine, and E. Bonucci. 1985. Osteonectin and Gla-protein in calf bone: ultrastructural immunohistochemical localization using the Protein A-gold method. *Calcif. Tissue Int.* 37:684–686.

Bianco, P., M. Costantini, L.C. Dearden, and E. Bonucci. 1988. Alkaline phosphatase positive precursors of adipocytes in the human bone marrow. *Br. J. Haematol.* 68:401–403.

Bianco, P., S.A. Kuznetsov, M. Riminucci, L.W. Fisher, A.M. Spiegel, and P.G. Robey. 1998. Reproduction of human fibrous dysplasia of bone in immunocompromised mice by transplanted mosaics of normal and Gs alpha-mutated skeletal progenitor cells. *J. Clin. Invest.* 101:1737–1744.

Bianco, P., M. Riminucci, S. Kuznetsov, and P.G. Robey. 1999. Multipotential cells in the bone marrow stroma: regulation in the context of organ physiology. *Crit. Rev. Eukaryot. Gene Expr.* 9:159–173.

Bradbeer, J.N., M. Riminucci, and P. Bianco. 1994. Giemsa as a fluorescent stain for mineralized bone. *J. Histochem. Cytochem.* 42:677–680.

Calvi, L.M., N.A. Sims, J.L. Hunzelman, M.C. Knight, A. Giovannetti, J.M. Saxton, H.M. Kronenberg, R. Baron, and E. Schipani. 2001. Activated parathyroid hormone/parathyroid hormone-related protein receptor in osteoblastic cells differentially affects cortical and trabecular bone. *J. Clin. Invest.* 107:277–286.

Calvi, L.M., G.B. Adams, K.W. Weibrecht, J.M. Weber, D.P. Olson, M.C. Knight, R.P. Martin, E. Schipani, P. Divieti, F.R. Bringhurst, et al. 2003. Osteoblastic cells regulate the haematopoietic stem cell niche. *Nature.* 425:841–846.

Chailakhyan, R.K., U.V. Gerasimov, and A.J. Friedenstein. 1978. Transfer of bone marrow microenvironment by clones of stromal mechanocytes. *Bull. Exp. Biol. Med.* 86:1633–1635.

Corsi, A., M.T. Collins, M. Riminucci, P.G. Howell, A. Boyde, P.G. Robey, and P. Bianco. 2003. Osteomalacic and hyperparathyroid changes in fibrous dysplasia of bone: core biopsy studies and clinical correlations. *J. Bone Miner. Res.* 18:1235–1246.

Damien, C.J., and J.R. Parsons. 1991. Bone graft and bone graft substitutes: a review of current technology and applications. *J. Appl. Biomater.* 2:187–208.

de Crombrugghe, B., V. Lefebvre, and K. Nakashima. 2001. Regulatory mechanisms in the pathways of cartilage and bone formation. *Curr. Opin. Cell Biol.* 13:721–727.

Friedenstein, A.J. 1980. Stromal mechanisms of bone marrow: cloning in vitro and retransplantation in vivo. *Hamatol. Bluttransfus.* 25:19–29.

Friedenstein, A.J. 1990. Bone marrow osteogenic stem cells. *In* Calcium Regulation and Bone Metabolism. D.V. Cohn, F.H. Glorieux, and T.J. Martin, editors. Elsevier, Cambridge, UK. 353–361.

Friedenstein, A.J., R.K. Chailakhyan, N.V. Latsinik, A.F. Panasyuk, and I.V. Keiliss-Borok. 1974. Stromal cells responsible for transferring the microenvironment of the hemopoietic tissues. Cloning in vitro and retransplantation in vivo. *Transplantation.* 17:331–340.

Holmbeck, K., P. Bianco, J. Caterina, S. Yamada, M. Kromer, S.A. Kuznetsov, M. Mankani, P.G. Robey, A.R. Poole, I. Pidoux, et al. 1999. MT1-MMP-deficient mice develop dwarfism, osteopenia, arthritis, and connective tissue disease due to inadequate collagen turnover. *Cell.* 99:81–92.

Karaplis, A.C., A. Luz, J. Glowacki, R.T. Bronson, V.L. Tybulewicz, H.M. Kronenberg, and R.C. Mulligan. 1994. Lethal skeletal dysplasia from targeted disruption of the parathyroid hormone-related peptide gene. *Genes Dev.* 8:277–289.

Krebsbach, P.H., S.A. Kuznetsov, K. Satomura, R.V. Emmons, D.W. Rowe, and P.G. Robey. 1997. Bone formation in vivo: comparison of osteogenesis by transplanted mouse and human marrow stromal fibroblasts. *Transplantation.* 63:1059–1069.

Kuznetsov, S., and P. Gehron Robey. 1996. Species differences in growth requirements for bone marrow stromal fibroblast colony formation in vitro. *Calcif. Tissue Int.* 59:265–270.

Kuznetsov, S.A., P.H. Krebsbach, K. Satomura, J. Kerr, M. Riminucci, D. Benayahu, and P.G. Robey. 1997. Single-colony derived strains of human marrow stromal fibroblasts form bone after transplantation in vivo. *J. Bone Miner. Res.* 12:1335–1347.

Lanske, B., A.C. Karaplis, K. Lee, A. Luz, A. Vortkamp, A. Pirro, M. Karperien, L.H. Defize, C. Ho, R.C. Mulligan, et al. 1996. PTH/PTHrP receptor in early development and Indian hedgehog-regulated bone growth. *Science.* 273:663–666.

Lee, K., J.D. Deeds, A.T. Bond, H. Juppner, A.B. Abou-Samra, and G.V. Segre. 1993. In situ localization of PTH/PTHrP receptor mRNA in the bone of fetal and young rats. *Bone.* 14:341–345.

Lee, K., J.D. Deeds, S. Chiba, M. Un-No, A.T. Bond, and G.V. Segre. 1994. Parathyroid hormone induces sequential c-fos expression in bone cells in vivo: in situ localization of its receptor and c-fos messenger ribonucleic acids. *Endocrinology.* 134:441–450.

Morrison, S.J., N. Uchida, and I.L. Weissman. 1995. The biology of hematopoietic stem cells. *Annu. Rev. Cell Dev. Biol.* 11:35–71.

Owen, M., and A.J. Friedenstein. 1988. Stromal stem cells: marrow-derived osteogenic precursors. *Ciba Found. Symp.* 136:42–60.

Riminucci, M., L.W. Fisher, A. Shenker, A.M. Spiegel, P. Bianco, and P. Gehron Robey. 1997. Fibrous dysplasia of bone in the McCune-Albright syndrome: abnormalities in bone formation. *Am. J. Pathol.* 151:1587–1600.

Riminucci, M., B. Liu, A. Corsi, A. Shenker, A.M. Spiegel, P.G. Robey, and P. Bianco. 1999. The histopathology of fibrous dysplasia of bone in patients with activating mutations of the *Gsα* gene: site-specific patterns and recurrent histological hallmarks. *J. Pathol.* 187:249–258.

Satomura, K., P. Krebsbach, P. Bianco, and P. Gehron Robey. 2000. Osteogenic imprinting upstream of marrow stromal cell differentiation. *J. Cell. Biochem.* 78:391–403.

Schipani, E., K. Kruse, and H. Juppner. 1995. A constitutively active mutant PTH-PTHrP receptor in Jansen-type metaphyseal chondrodysplasia. *Science.* 268:98–100.

Schipani, E., C.B. Langman, A.M. Parfitt, G.S. Jensen, S. Kikuchi, S.W. Kooh, W.G. Cole, and H. Juppner. 1996. Constitutively activated receptors for parathyroid hormone and parathyroid hormone-related peptide in Jansen's metaphyseal chondrodysplasia. *N. Engl. J. Med.* 335:708–714.

Schipani, E., B. Lanske, J. Hunzelman, A. Luz, C.S. Kovacs, K. Lee, A. Pirro, H.M. Kronenberg, and H. Juppner. 1997. Targeted expression of constitutively active receptors for parathyroid hormone and parathyroid hormone-related peptide delays endochondral bone formation and rescues mice that lack parathyroid hormone-related peptide. *Proc. Natl. Acad. Sci. USA.* 94:13689–13694.

Sherley, J.L. 2002. Asymmetric cell kinetics genes: the key to expansion of adult stem cells in culture. *Stem Cells.* 20:561–572.

Streeter, G. 1949. Developmental horizons in human embryos. *Contributions to Embryology.* 33:151–167.

Tavassoli, M., and J.M. Yoffey. 1983. Bone Marrow: Structure and Function. Alan R. Liss, Inc., New York. 300 pp.

Watt, F.M., and B.L. Hogan. 2000. Out of eden: stem cells and their niches. *Science.* 287:1427–1430.

Westen, H., and D.F. Bainton. 1979. Association of alkaline-phosphatase-positive reticulum cells in bone marrow with granulocytic precursors. *J. Exp. Med.* 150:919–937.